Faculty and Researchers   Faculty and Researchers' Publications

2014-09-28

High power laser heating of low absorption materials

Olson, K.; Talghader, J.; Ogloza, A.; Thomas, J.

American Institute of Physics (AIP)

High power laser heating of low absorption materials

K. Olson,[1] A. Ogloza,[2] J. Thomas,[3] and J. Talghader[1,a)]

[1]*Electrical Engineering, University of Minnesota, Minneapolis, Minnesota 55455, USA*
[2]*Naval Postgraduate School, 1 University Cir, Monterey, California 93943, USA*
[3]*Electro Optics Center, Pennsylvania State University, 222 Northpointe Blvd., Freeport, Pennsylvania 16229, USA*

A model is presented and confirmed experimentally that explains the anomalous behavior observed in continuous wave (CW) excitation of thermally isolated optics. Distributed Bragg Reflector (DBR) high reflective optical thin film coatings of HfO_2 and SiO_2 were prepared with a very low absorption, about 7 ppm, measured by photothermal common-path interferometry. When illuminated with a 17 kW CW laser for 30 s, the coatings survived peak irradiances of 13 MW/cm^2, on 500 μm diameter spot cross sections. The temperature profile of the optical surfaces was measured using a calibrated thermal imaging camera for illuminated spot sizes ranging from 500 μm to 5 mm; about the same peak temperatures were recorded regardless of spot size. This phenomenon is explained by solving the heat equation for an optic of finite dimensions and taking into account the non-idealities of the experiment. An analytical result is also derived showing the relationship between millisecond pulse to CW laser operation where (1) the heating is proportional to the laser irradiance (W/m^2) for millisecond pulses, (2) the heating is proportional to the beam radius (W/m) for CW, and (3) the heating is proportional to W/m $\cdot$ $\tan^{-1}(\sqrt{t}/m)$ in the transition region between the two. © *2014 AIP Publishing LLC.*
[http://dx.doi.org/10.1063/1.4896750]

I. INTRODUCTION

The study of laser interactions with materials has primarily developed using ultra-short pulsed lasers.[1–4] However, many applications of laser heating involve continuous wave (CW) lasers,[5–8] and their corresponding thermal material damage mechanisms are poorly understood. In previous research, there have been seeming anomalies in the temperature distributions seen under CW excitation.[5,6,9] In this paper, a model for high power CW heating of very low absorption mirrors is developed and tested that explains these anomalies.

Solutions to the steady state laser heating problem were developed throughout the 1970s and 80s.[6,10–12] This work modeled nonlinear absorption, reflection, density, specific heat, and thermal conductivity.[6,11] It is our goal to expand these derivations to include thermal loading into a single equation covering the time scale from millisecond pulses to steady state solutions. We are also interested in the general relationship between incident power, material properties, and duration of pulse as they affect the temperature rise of an optic.

II. HEAT EQUATION SOLUTION WITH HEAT GENERATION TERM

Our motivation for the following derivation was that a simple and fast 3D numerical model was not available to us for CW laser illumination on high reflectivity optics. Many of the simple numerical models required time steps that were too short to retain stability and simulate for more than a few milliseconds. In general, the solution to the laser heating problem comes from solving the partial differential heat equation with linear thermal properties.

$$\frac{\partial T}{\partial t} = \alpha \nabla^2 T + \frac{q(r,z,t)}{\rho c}. \tag{1}$$

T is the temperature profile in cylindrical coordinates. We will take the laser beam to be cylindrically symmetric, eliminating the θ term. α is the thermal diffusivity, q(r,z,t) is the generated heat term, ρ is the density, and c is the specific heat. To solve this equation, we first solve for a uniform energy pulse in radius and a delta function in depth (z) and time (t). This solution is readily available and is given below for the boundary conditions $T|_{z=\infty} = T_0$ and $dT/dz|_{z=0} = 0$ (Refs. 13 and 14)

$$T(z,t) = T_0 + \frac{E/A}{\rho c \sqrt{\pi \alpha t}} e^{\left(\frac{-z^2}{4\alpha t}\right)}$$
$$\frac{\Delta T(z,t)}{\Delta T_C} = \frac{T(z,t) - T_0}{\Delta T_C} = \frac{1}{\sqrt{\pi \alpha t}} e^{\left(\frac{-z^2}{4\alpha t}\right)}. \tag{2}$$

Here, $\Delta T_C = E/(A\rho c)$ and is the characteristic temperature scale, where E/A is the total energy per unit area delivered in the pulse. In this solution, it is also assumed that the total energy of the pulse exists in the semi-infinite domain $0 \leq z \leq \infty$ at all times.

Next, we solve for the dissipation of a Gaussian temperature profile in a one dimensional cylinder. We can solve this problem using separation of variables and Fourier analysis to get the following well-known result:[13,14]

---

a)Author to whom correspondence should be addressed. Electronic mail: joey@umn.edu.

$$\frac{\Delta T(r,t)}{\Delta T_C} = \frac{1}{2\pi w(t)^2} e^{\left(\frac{-r^2}{2w(t)^2}\right)} \tag{3a}$$

$$w(t)^2 = w^2 + 2\alpha t. \tag{3b}$$

Now $\Delta T_C = E/(L\rho c)$, w is half of the laser pulse beam width, and w(t) represents how the temperature profile width changes over time assuming a 2D Gaussian laser profile.

We can find the 3D solution to the heat equation for an infinitely fast Gaussian laser pulse that is completely absorbed at the surface ($z = 0$) by combining the two solutions of Eqs. (2) and (3a) using product solution. In the final solution, $\Delta T_C = E/\rho c$ and is used to convert the diffusion profiles to temperature from the energy input to the system

$$\Delta T(r,z,t) = \frac{E}{2\pi^{3/2}\rho c\sqrt{\alpha}} \frac{e^{\left(\frac{-r^2}{2w^2+4\alpha t}\right)} e^{\left(\frac{-z^2}{4\alpha t}\right)}}{\sqrt{t}(w^2+2\alpha t)}, \tag{4}$$

where E is the total energy of the laser pulse. Equation (4) gives a very nice analytical expression for the diffusion of a Gaussian energy pulse but it is not valid for a CW laser where the pulse duration is long enough that the temperature can diffuse while the laser is still on. In the past, the heat equation (1) has been solved for very long duration pulses ($t = \infty$) and very short pulses ($t \ll w^2/2\alpha$),[8–12] whereas we provide a solution for all times. A first simplification is that in a small increment of time, the energy can be replaced with a power multiplied by time. This power is the fraction of the power of the laser multiplied by the absorption of the surface

$$E = \eta P_{Laser}\Delta t = P_{absorbed}\Delta t, \tag{5}$$

where η is the fraction of laser power that is absorbed at the surface and Δt is the duration of the pulse. Now plugging 5 into 4 and taking the limit where Δt goes to dt and integrating over the duration of the pulse we get an expression for the time-dependent heating of a CW laser.

$$\Delta T(r,z,t) = \frac{P_{absorbed}}{2\pi^{3/2}\rho c\sqrt{\alpha}} \times \int_0^t \frac{e^{\left(\frac{-r^2}{2w^2+4\alpha t'}\right)} e^{\left(\frac{-z^2}{4\alpha t'}\right)}}{\sqrt{t'}(w^2+2\alpha t')} dt', \tag{6}$$

where t is the total time the CW laser power is applied to the optical surface. Equation (6) integrates over all the infinitesimally short pulses and allows them to diffuse for t' seconds. At the point where r is zero the maximum power of the laser is incident on the surface ($z = 0$), it is this point where material changes and damage will most likely first occur. To solve this equation analytically, we can take r to be zero and t to be infinite to get the z dependence at steady state, or r and z to be 0 to get the time dependence at the location of maximum temperature. The point of maximum temperature is of particular interest in laser damage testing as it is likely the location of damage initiation

$$\Delta T(0,z,\infty) = \frac{P_{absorbed}}{kw2\sqrt{2\pi}} e^{\left(\frac{z^2}{2w^2}\right)} \mathrm{erf}\left(\frac{|z|}{w\sqrt{2}}\right) \tag{7}$$

$$\Delta T(0,0,t) = \frac{P_{absorbed}}{kw\pi\sqrt{2\pi}} \tan^{-1}\left(\frac{\sqrt{2\alpha t}}{w}\right), \tag{8}$$

where erf(x) is the error function and is defined as the integral of the Gaussian distribution from 0 to x with a leading factor of $2/\sqrt{\pi}$, and k is the thermal conductivity. Note that $\alpha = k/c\rho$. Notice that if $t \ll w^2/2\alpha$ signifying a short pulse, then the $\tan^{-1}$ can be approximated by the small angle theorem and gives the following:

$$\Delta T(0,0,t) \cong \frac{P_{absorbed}}{w^2} \frac{\sqrt{\alpha t}}{k\pi^{3/2}}. \tag{9}$$

We can also simplify equation (8) for long duration pulses ($t = \infty$)

$$\Delta T(0,0,\infty) = \Delta T_{max} = \frac{P_{absorbed}}{w} \frac{1}{k2\sqrt{2\pi}}. \tag{10}$$

Equations (9) and (10) agree with previous publications[8,10–12] and show that for short duration pulses the temperature rise is dependent on irradiance and scales as the inverse of the beam area ($1/m^2$), and for longer pulses scales as the inverse of the beam radius ($1/m$). Equation (8) defines how the system behaves at all times. The time when Eq. (9) becomes invalid can be found by using the small angle approximation of $\tan^{-1}$, to at least 1% accuracy we require the condition

$$t < 0.01527 \frac{w^2}{\alpha}. \tag{11}$$

For SiO_2 with a laser beam radius of $w = 0.5$ mm, the condition is $t < 5$ ms. This shows that for CW laser heating of low absorption optics, the temperature rise does not depend on the irradiance of the laser (W/m^2) but on the inverse of the laser beam radius (W/m). To approximate the $\tan^{-1}$ function to 1% accuracy for large angles requires that

$$t > 2026.1 \frac{w^2}{\alpha}. \tag{12}$$

Another important solution to the laser heating problem is cooling by self-quenching, where the bulk material is a heat sink, after the laser is off. To find this solution without taking into account any convective losses, we need to integrate Eq. (6) from t to $t + t_p$ where t_p is the duration of the pulse

$$\Delta T(r,z,t) = \frac{P_{absorbed}}{2\pi^{3/2}\rho c\sqrt{\alpha}} \times \int_t^{t+t_p} \frac{e^{\left(\frac{-r^2}{2w^2+4\alpha t'}\right)} e^{\left(\frac{-z^2}{4\alpha t'}\right)}}{\sqrt{t'}(w^2+2\alpha t')} dt'. \tag{13}$$

Equation (13) integrates over all the infinitesimally small pulses but allows each pulse to diffuse for an extra amount of time t. If we take the limit as $t \to 0$, then we recover Eq. (6). To solve Eq. (13) analytically, we take r and z to be 0 and get the result below. We have also replaced t with $t - t_p$ and enforced the rule $t \ge t_p$ to give real results

$$\Delta T(0,0,t) = \frac{P_{absorbed}}{kw\pi\sqrt{2\pi}}$$
$$\times \left(\tan^{-1}\frac{w}{\sqrt{2\alpha(t-t_p)}} - \tan^{-1}\frac{w}{\sqrt{2\alpha t}} \right). \quad (14)$$

III. EXPERIMENT

We confirmed our model experimentally by measuring the surface temperature of an ultra-low absorbing optical thin film which was exposed to high power CW laser light. We measured the optical surface absorption using Photothermal Common-Path Interferometry (PCI) and observed an average absorption of 7 ppm for HfO_2/SiO_2 high reflectivity Distributed Bragg Reflectors (DBRs) and <1 ppm for Ta_2O_5/SiO_2 DBRs. The DBRs were tuned to have a peak reflectivity at a wavelength of 1.064 μm. The laser was a 17 kW CW Ytterbium doped IPG photonics YLS-1700 laser. The laser is capable of emitting 0.880 kW to 15.5 kW reliably and can focus to a spot size ranging from 0.5 mm to 7.2 mm, resulting in an irradiance range of 6.32×10^{-4} to 13.3 MW/cm^2.

The optic is slightly misaligned so that the beam is reflected back to an absorbing carbon block. If the optical coating fails, the laser propagates through the optic into an integrating sphere automatically shutting down the laser.

Prior to testing each optic, both surfaces were cleaned on the front and back sides by drag wiping with a lens tissue using a drop of methanol as the solvent. The tissue was only used once, and up to three drag wipes were performed on each side of the optic to be tested.

In cases where the optics did not fail, we measured the spatial surface temperature distribution using an infrared camera capable of measuring a temperature range from 0 to 250 °C at a 30 Hz frame rate. The optics were placed on a motorized XY stage to automate testing. The optics under test were SiO_2 optical flats, 1 in. in diameter and 0.25 in. thick, or 1 in. Si wafers. The substrates were coated with HfO_2/SiO_2 or Ta_2O_5/SiO_2 DBR coatings. Because the Ta_2O_5/SiO_2 DBRs had extremely low absorption properties (<1 ppm), the camera could not reliably measure the temperature rise during a laser shot, so the data presented here concentrate on the HfO_2/SiO_2 coatings. In Figure 1, the experimental setup of the laser and beam path is shown.

Each individual optic was tested either to avoid laser conditioning (the slow strengthening of an optical element by exposing it to gradually increasing intensities of laser
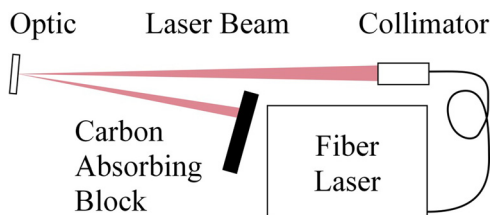

FIG. 1. Experimental setup with beam path added for clarity. The reflective optic is slightly misaligned to send the reflected beam to an absorbing carbon block.
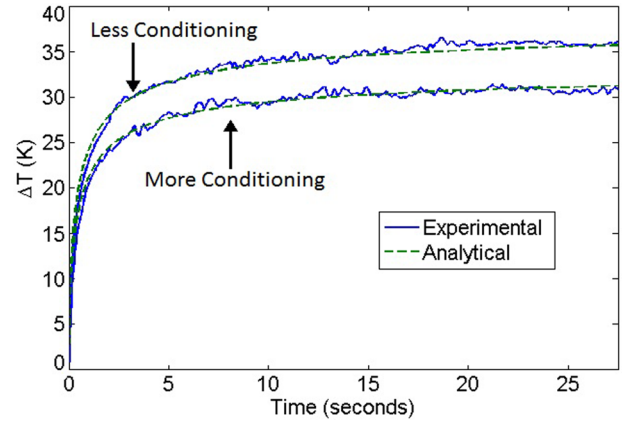

FIG. 2. Laser heating of SiO_2 1 in. optical flat with HR HfO_2/SiO_2 DBR coating. $P_{laser} = 15.5$ [kW], w = .55 [mm], c = 522 [J/(kg K)], $\rho = 5710$ [kg/m^3], k = 1.02 [W/(m K)], $\alpha = 3.43 \times 10^{-7}$ [m^2/s]. The thermal properties are an average of the materials within the film.

light) or to intentionally condition the optic. There were 9 testing sites on each optic; at the first site, 10 shots were completed in succession to condition the optic. As we moved through the sites fewer successive shots were performed (to vary the level of conditioning) until at the 9th site, only the highest power density was used. In Figure 2, the experimental maximum change in temperature versus time is compared with the analytical result of Eq. (8). The shot showing a lower thermal rise was conditioned with one extra shot at 70% power, reducing the average absorption by 12.9% from 7 ppm to 6.1 ppm. The drop in absorption was not able to be confirmed by PCI measurements so we cannot be certain that this change was from conditioning. The thermal properties used in the analytical result were a volumetric average of the materials within the film.

We were also able to test multiple laser spot sizes at different locations on the optic. In Figure 3, we show how the analytical result fits with varying spot sizes. Notice that although the larger spot size produces less heating, the model shows that there is more absorption. In the next section, we discuss non-ideal conditions and see if the absorption results in Figure 3 were real or due to other effects.
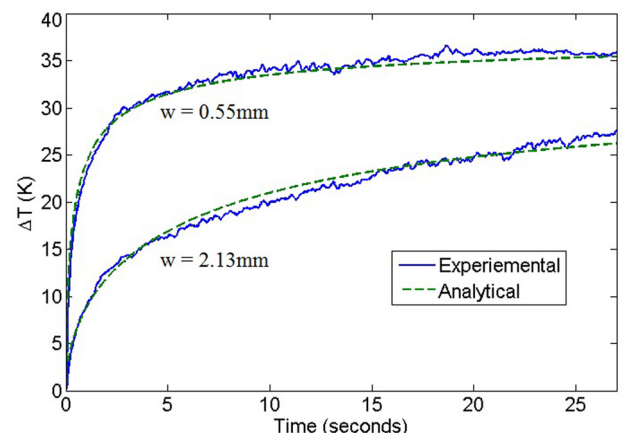

FIG. 3. Laser heating comparison of differing spot sizes. For (w = 0.55 mm) absorption = 14 ppm, and (w = 2.13 mm) absorption = 26 ppm.

IV. NON-IDEAL EFFECTS

The data closely followed the model as shown, but there are a few experimental non-idealities we would like to address. First, the optic under laser illumination is not infinite in radius and semi-infinite in z, second, the resolution of the thermal camera is not infinite, and, third, the optic has additional thermal losses besides diffusion. Constraining the diffusion to finite dimensions requires the use of an insulating boundary condition. Without defining these boundary conditions, we can solve the problem by using the result from the infinite case and summing the results offset by twice the distance to the boundary producing a solution that satisfies the boundary conditions.[13,14] This process can be thought of the diffusion being reflected at the boundaries so that nothing diffuses outside of the boundaries

$$\Delta T(z,t) = \frac{E/A}{\rho c L} \vartheta_3 \left(\frac{\pi z}{2L}, e^{\left(\frac{-\pi^2 t \alpha}{L^2}\right)} \right)$$

$$\Delta T(z=0,t) = \frac{E/A}{\rho c \sqrt{\pi \alpha t}} \vartheta_3 \left(0, e^{\left(\frac{-L^2}{\alpha t}\right)} \right) \tag{15}$$

$$\Delta T(r,t) = \frac{\frac{E}{L} \vartheta_3 \left(\frac{\pi r}{2R}, e^{\left(\frac{-\pi^2 (w^2+2\alpha t)}{2R^2}\right)} \right)}{\rho c 2R \sqrt{2\pi(w^2+2\alpha t)}},$$

$$\Delta T(r=0,t) = \frac{\frac{E}{L} \vartheta_3 \left(0, e^{\left(\frac{-2R^2}{w^2+2\alpha t}\right)} \right)}{\rho c 2\pi(w^2+2\alpha t)} \tag{16}$$

where ϑ_3 is the Jacobi Theta function of the third kind and is essentially an infinite sum of exponential functions each offset from each other by either 2L or 2R. Combining Eqs. (15) and (16) and integrating over time we get a new expression for the laser heating response

$$\Delta T(r=0, z=0, t) = \frac{P_{absorbed}}{2\pi^{3/2} \rho c \sqrt{\alpha}}$$

$$\times \int_0^t \frac{\vartheta_3 \left(0, e^{\left(\frac{-L^2}{\alpha t}\right)} \right) \vartheta_3 \left(0, e^{\left(\frac{-2R^2}{w^2+2\alpha t}\right)} \right)}{\sqrt{t'}(w^2+2\alpha t')} dt'. \tag{17}$$

This equation no longer has an analytical result and does not converge to a finite temperature as $t \rightarrow \infty$. However, Eq. (17) more accurately depicts CW laser heating when solved numerically compared to Eq. (6) when L is small compared to the diffusion length $\sqrt{\alpha t}$ or R is small compared to Gaussian width $(w^2 + 2\alpha t')$. It is also important to note that Eq. (17) will most likely be needed to model the situation where a suspended film is being illuminated by laser light.

Suspended films should have low laser damage thresholds (LDTs) because of the relatively rapid (nanoseconds) heating of the surface, which diffuses almost instantaneously to the other side of the film. Once this happens, there is nowhere for the heat to go and the film will indefinitely heat up until damage or another thermal loss mechanism takes over, such as radiation or conduction through the suspended film supports. We were able to see a similar situation by illuminating films deposited on 1 in. diameter and 0.5 mm thick silicon wafers.

The Si wafer has about 2 orders of magnitude higher thermal conductivity than glass substrates and is much thinner allowing the heat to dissipate to the back side of the optic.

We show in Figure 4 both experimentally and theoretically that a finite R and L can greatly change the temperature response at the surface compared to the analytical result of Eq. (8). The two experimental results are measurements of the same optic under the same laser illumination and conditioning state, but at different locations on the optic. Still the only fitting parameter is the absorption at the surface, and we found that on Si the films were 2 to 3 times more absorptive. The absorption of these films could not be directly measured with PCI due to the interfering effects of the absorptive Si substrate.

In Figure 4, we use the substrate material parameters in the model rather than a volumetric average of the film as in Figures 2 and 3. Previously, the substrate was similar to the film and the thermal conductivity was low so that much of the thermal energy existed in the film and near the surface, now with a higher thermal conductivity in the substrate more of the thermal energy exists within the substrate and thus we use the substrate material parameters. At shorter illumination times, from Figure 4, it appears that the experiment showed less heating than expected and at longer illumination times it matches the calculations. This could be because we have not taken into account the much lower thermal conductivity of the surface film absorbing the laser at short times, and at larger times the heat is sufficiently diffused into the Si substrate so that the experiment is closer to the modeled case. It appears that the cooling after the laser is off is also losing heat more slowly than expected from the model. The maximum temperature change is much lower on Si substrates than on SiO$_2$ substrates but Eq. (17) predicts that the absorption is actually higher for the films on Si substrates. The higher absorption values are likely due to light leakage through the high reflective coating into the substrate. The DBR transmission is approximately 10 to 20 ppm with the
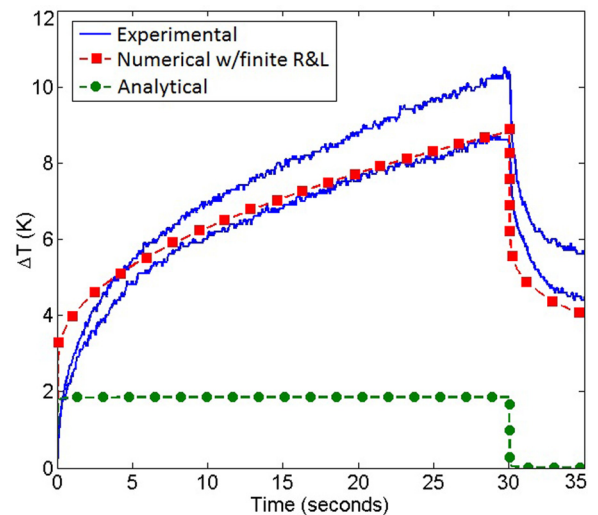

FIG. 4. Laser heating of Si wafer with HR HfO$_2$/SiO$_2$ DBR coating. P$_{laser}$ = 15.3 [kW], absorption = 25 [ppm], w = .275 [mm], c = 705 [J/(kg K)], ρ = 2329 [kg/m^3], k = 149 [W/(m K)], α = 9.07 $\times$ 10^{-5} [m^2/s], R = 12.7 [mm], L = 0.5 [mm]. The analytical curve shows the prediction for a semi-infinite optic (i.e., one with low thermal conductivity as in Eqs. (8) and (13) and Figures 2 and 3.).

remaining power absorbed in the substrate causing the increase in absorption.

To take into account the resolution of the thermal camera, we can average Eq. (16) over the area of a pixel located at the center of the laser beam. Noticing $r^2 = x^2 + y^2$, we can easily average over a square pixel area. We also assume that $R \gg (w^2 + 2\alpha t)$ so that the Jacobi Theta function reduces back to a Gaussian

$$\frac{1}{Area} \int\int_{Square} e^{\left(\frac{-r^2}{2w^2 + 4\alpha t}\right)} r\,dr\,d\theta$$

$$= \frac{1}{P_s^2} \int\int_{\frac{-P_s}{2}}^{\frac{P_s}{2}} e^{\left(\frac{-x^2 - y^2}{2w^2 + 4\alpha t}\right)} dx\,dy$$

$$= \frac{2\pi(w^2 + 2\alpha t)}{P_s^2} \operatorname{erf}\left(\frac{P_s}{2\sqrt{2(w^2 + 2\alpha t)}}\right)^2. \qquad (18)$$

In Eq. (18), P_s is the length of the side of a pixel in the thermal camera. Substituting Eq. (18) into (17), we will get our final model for laser heating

$$\Delta T(0, z, t) = \frac{P_{absorbed}}{P_s^2 \rho c \sqrt{\pi\alpha}} \times \int_0^t \frac{\vartheta_3\left(0, e^{\left(\frac{-L^2}{\alpha t}\right)}\right) \vartheta_3\left(0, e^{\left(\frac{-2R^2}{w^2 + 2\alpha t}\right)}\right)}{\sqrt{t'}}$$

$$\times \operatorname{erf}\left(\frac{P_s}{2\sqrt{2(w^2 + 2\alpha t')}}\right)^2 dt'. \qquad (19)$$

With Eq. (19), we can explain why experiments at spot sizes below the pixel resolution did not show an increase in the maximum temperature reading with decreasing spot size. With a spot size of w = 0.15 mm and a laser power of 15.5 kW (an 8 times higher irradiance than that of the shots in Figure 2, with the same optic), a temperature rise of about 17 K was seen. The thermal camera in this experiment was placed sufficiently far enough away to produce a pixel size of $P_s = 2$ mm. From these data, we can see in Figure 5 that the actual tem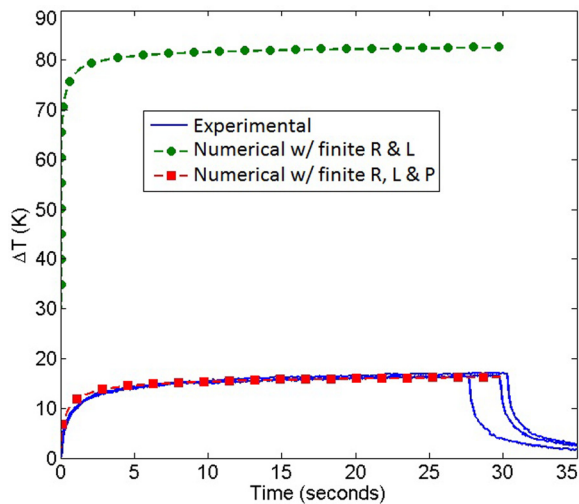perature rise of the optic was probably around 85 K, about 5 times hotter than recorded by the thermal camera in all 3 successive shots. The 3 experimental results shown in Figure 5 are laser shots on the same optic and at the same laser power with different pulse durations at 3 different locations.

From Figure 5, we can see that having a pixel size much greater than the laser beam width can result in very different readings from what actually occurred. The model also provides a method to extract an accurate reading of absorption regardless of experimental parameters. The final model of Eq. (17) with all experimental corrections can fit experiments with all spot sizes without varying absorption as was done in the previous models in Figures 2, 3, and 4.

V. CONCLUSION

We presented and confirmed an analytical and numerical model for the thermal heating of low absorption materials under laser illumination. The model should be correct for thermal time scales and was tested and confirmed by CW laser heating experiments. For CW laser heating, the most important results are Eqs. (8) through (10), showing that thermal heating is dependent on the inverse of the beam radius of the laser (W/m) when in the long pulse regime. For materials with a high thermal diffusivity, the equilibrium temperature produced by laser heating can be reached in seconds, and for the short pulse regime in milliseconds. When reporting laser damage thresholds of materials with CW lasers, this work shows that in many cases, the threshold should be reported in terms of the laser power scaled by the inverse of the beam radius rather than in terms of the irradiance of the laser.

ACKNOWLEDGMENTS

FIG. 5. Laser heating of SiO_2 1 in. optical flat with HR HfO_2/SiO_2 DBR coating and non-ideal thermal camera properties. $P_{laser} = 15.5$ [kW], absorption = 6 [ppm], w = .15 [mm], c = 703 [J/(kg K)], $\rho = 2648$ [kg/m^3], k = 1.5 [W/(m K)], $\alpha = 8.06 \times 10^{-7}$ [m^2/s], $P_s = 2$ mm.

[1]S. Moradi, S. Kamal, P. Englezos, and S. G. Hatzikiriakos, Nanotechnology **24**, 415302 (2013).
[2]R. Stoian, A. Rosenfeld, D. Ashkenasi, I. Hertel, N. M. Bulgakova, and E. E. B. Campbell, Phys. Rev. Lett. **88**, 097603 (2002).
[3]M. D. Shirk and P. A. Molian, J. Laser Appl. **10**, 18 (1998).
[4]J. H. Bechtel, J. Appl. Phys. **46**, 1585 (1975).
[5]S. Bodea and R. Jeanloz, J. Appl. Phys. **65**, 4688 (1989).
[6]M. Yamada, K, Nambu, Y. Itoh, and K. Yamamoto, J. Appl. Phys. **59**, 1350 (1986).
[7]M. Stoneback, A. Ishimaru, C. Reinhardt, and Y. Kuga, Opt. Eng. **52**, 036001 (2013).
[8]Y. Tian, G. Li, B. Q. Yao, and Y. Z. Wang, Appl. Phys. B. **103**, 107 (2011).
[9]R. M. Wood, Opt. Laser Technol. **29**, 517 (1998).
[10]M. Lax, J. Appl. Phys. **48**, 3919 (1977).
[11]M. Lax, Appl. Phys. Lett. **33**, 786 (1978).
[12]E. Liarokapis and Y. S. Raptis, J. Appl. Phys. **57**, 5123 (1985).
[13]H. B. Fischer, E. J. List, R. C. Y. Koh, J. Imberger, and N. H. Brooks, *Mixing in Inland and Coastal Waters* (Academic Press, MA, 1979).
[14]S. A. Socolofsky and G. H. Jirka, *Environmental Fluid Mechanics 1: Mixing and Transport Processes in the Environment* (Texas A&M University, Texas, 2005) pp. 37–39.